Article

Not peer-reviewed version

# Alginate–Chitosan Biopolymer Nanoparticles for Efficient Bacteriophage Encapsulation and Transport

Patricia Dolores Martinez-Flores , Joselyn Aime García-Mar , Jose Manuel García-Perez , David Encinas-Basurto , Gerardo García-González , Gerardo Rodea , Marco Antonio López Mata , Antonio Topete , Josué Juárez *

Posted Date: 27 February 2026

doi: 10.20944/preprints202602.1251.v1

Keywords: bacteriophage; alginate-chitosan nanoparticles; polyelectrolyte complexation

 doi:10.20944/preprints202602.1251.v1



*Article*

# Alginate–Chitosan Biopolymer Nanoparticles for Efficient Bacteriophage Encapsulation and Transport

**Patricia Dolores Martínez-Flores [1], Joselyn Aime García-Mar [1], Jose Manuel García-Perez [2], David Encinas-Basurto [1], Gerardo García-González [2], Gerardo Rodea [3], Marco Antonio López Mata [4], Antonio Topete [5] and Josué Juárez [1,*]**

[1] Departamento de Física, Facultad de Ciencias Exactas y Naturales, Universidad de Sonora, Hermosillo CP 83000, Mexico

[2] Departamento de Microbiología, Facultad de Medicina y Hospital Universitario "Dr. José Eleuterio González", Universidad Autónoma de Nuevo León, Monterrey 64460, NL., Mexico

[3] Laboratorio de Investigación en Microbiología y Resistencia Bacteriana, Hospital infantil de México, Federico Gómez, Ciudad de México, 06720, Mexico

[4] Departamento de Ciencias de la Salud, Facultad Interdisciplinaria de Ciencias Biológicas y de Salud, Universidad de Sonora, Cajeme CP 85010, Mexico

[5] Departamento de Física de Partículas, Instituto de Materiales e Instituto de investigación en Salud, Universidad de Santiago de Compostela, 15782 Santiago de Compostela, España

* Correspondence: josue.juarez@unison.mx

**Abstract**

**Background/Objectives**: The quest for effective therapeutic alternatives for infections caused by multidrug-resistant (MDR) bacteria remains a major global health priority. In this context, bacteriophage therapy has re-emerged as a promising strategy due to its high host specificity and ability to infect and lyse targeted bacterial strains. However, clinical translation is limited by biological and technological challenges, including phage instability and rapid inactivation after administration. Alginate- and chitosan-based polymeric nanomatrices offer a practical way to address these limitations. Properly engineered nanoparticles can improve phage stability, protect against environmental stressors, reduce inactivation, and enable localized, controlled release at the infection site. **Methods**: A polysaccharide-based nanocarrier composed of hydrophobically modified alginate (mAlg) and chitosan was developed. Encapsulation of bacteriophage vB_Eco_K-02 within mAlg-Cs nanoparticles was achieved by ultrasonication-assisted polyelectrolyte complexation. Particle size, ζP, and morphology were evaluated, and phage encapsulation efficiency and antibacterial activity were assessed in vitro. **Results**: The mAlg-Cs formulation at a 1:0.625 mass ratio yielded nanoparticles with the most favorable physicochemical properties, including improved size distribution, high colloidal stability, and regular morphology. vB_Eco_K-02-loaded NPs (mAlg-Cs-Phg) achieved a high encapsulation efficiency (99%) and preserved lytic activity after formulation, resulting in strong inhibition of *E. coli* growth in kinetic assays. **Conclusions**: mAlg-Cs nanoparticles provide an efficient platform for encapsulating vB_Eco_K-02 while preserving phage infectivity and enabling effective antibacterial activity. This nanosystem represents a promising strategy to enhance phage delivery for the treatment of bacterial infection.

**Keywords:** bacteriophage; alginate-chitosan nanoparticles; polyelectrolyte complexation

## 1. Introduction

One of the most relevant global health treats is infection caused by multidrug-resistant (MDR) bacteria. The emergence and spread of MDR strains have been driven largely by the prolonged misuse and overuse of antibiotics [1]. Patients with chronic pulmonary diseases, such as pneumonia, chronic obstructive pulmonary disease (COPD), bronchiectasis and cystic fibrosis (CF), represent

 doi:10.20944/preprints202602.1251.v1



major risk groups, as they frequently experience recurrent bacterial infections over short time intervals [2]. In these patients, eradication is particularly challenging because bacteria can deploy multiple resistance mechanisms, including reduced drug uptake, active efflux, enzymatic drug inactivation, and biofilm formation. Consequently, there is an urgent need to develop therapeutic strategies that can more effectively control bacterial infections.

In this context, bacteriophages therapy (phage therapy) has re-emerged as a promising alternative to, or adjunct to, conventional antibiotic treatment. In contrast to broad-spectrum antibiotics, phages show high host specificity and infect and lyse targeted bacterial strains [3]. A key advantage of this approach is its potential to eliminate pathogenic bacteria while largely preserving the patient's microbiota. However, phage therapy remains constrained by several biological and technological challenges. For example, phages are highly sensitive to environmental and physiological stressors, including temperature changes, pH extremes, enzymatic degradation, and host immune clearance, which can reduce therapeutic activity after administration [4,5]. As result, direct administration of free phages often leads to limited dose control, poor biodistribution, and insufficient residence time at the infection site.

Applied nanotechnology offers practical ways to address these limitations through the design of nanoparticle-based delivery systems. Properly engineered nanoparticles can improve phage stability, reduce inactivation, protect against environmental stressors, and enable localized, controlled release at target sites [6,7]. Among the biomaterials used to fabricate phage encapsulating nanoparticles, polysaccharides, particularly alginate and chitosan, are widely used due to their stability, biodegradability, biocompatibility, and low toxicity, which are critical for medical applications. Alginate is a naturally occurring anionic polysaccharide that readily form hydrogels in the presence of divalent cations, enabling efficient phage encapsulation while maintaining phage viability. In contrast, chitosan is a cationic polysaccharide derived from chitin that exhibits biocompatibility, biodegradability, intrinsic antimicrobial activity, and mucoadhesive properties, which can enhance localized delivery through interactions with biological tissues and mucus layers. Accordingly, alginate-chitosan-based matrices have been widely explored as versatile platforms for encapsulating therapeutic drugs, photosensitive agents, bioactive compounds, essential oils, and bacteriophages. For example, multifunctional alginate-chitosan nanosystems have been designed to co-encapsulate doxorubicin and indocyanine green (ICG) for combined chemo- and phototherapy applications [8]. Chitosan-alginate composites encapsulating thyme and garlic essential oils have shown enhanced bactericidal performance against foodborne pathogens [9]. Moreover, alginate-chitosan nanoparticles loaded with quercetin have demonstrated high encapsulation efficiency and improved antibacterial activity against *S. aureus* and *E. coli* [10]. In the context of cystic fibrosis pulmonary infections, alginate-chitosan nanoparticles have also been investigated as drug delivery systems capable of improving interaction with thickened mucus and enabling controlled release of therapeutics such as tobramycin, rifampicin, and ciprofloxacin [11,12]. Due to their biocompatibility and protective capacity, these systems have also been explored as encapsulation matrices that preserve phage infectivity during storage and transport while enabling release under relevant physiological conditions. Importantly, such formulations can enhance phage resistance to harsh environments and improve therapeutic performance, thereby broadening the range of feasible administration routes [6,13,14].

In this study, a polysaccharide-based nanosystem composed of hydrophobically modified alginate (mAlg) and chitosan was synthesized. Encapsulation of vB_Eco_K-02 within alginate–chitosan particles was achieved by polyelectrolyte complexation. The formulation was optimized by adjusting the pH of the alginate and chitosan solutions and the biopolymer mass ratio. The resulting nanoparticles were characterized by dynamic light scattering (DLS), zeta potential (ζP) measurements, and atomic force microscopy (AFM). Using the double-layer agar assay, mAlg-Cs nanoparticles showed high phage encapsulation efficiency (99%) and maintained a strongly negative surface charge consistent with colloidal stability (ζP = -42 mV). The antibacterial activity of phage-loaded mAlg-Cs NPs against an *Escherichia coli* strain isolated from cystic fibrosis patient was

 doi:10.20944/preprints202602.1251.v1



evaluated under different pH conditions (3.0, 7.4, 11.0) and incubation temperatures (37, 40, and 50 °C). Interestingly, under alkaline conditions (pH 11.0) at 37 °C, the mAlg-Cs NPs formulation markedly suppressed bacterial growth kinetics, supporting its potential as phage delivery platform for antibacterial therapy.

## 2. Materials and Methods

Sodium alginate (Alg, average molecular weight 26 kDa, M/G ratio 1.56), chitosan (Cs, low average molecular weight 120 kDa, 79% degree of deacetylation), 1-Decanol, sodium hydroxide, N,N-Dimethylformamide (DMF), Luria-Bertani (LB) broth all where from Sigma Aldrich. Agar-agar was from MCD LAB. Hydrochloric acid was from J.T. Baker. Spectra/Pro 1 dialysis Tubing, 6-8 kD MWCO, 23 mm flat width, 14.6mm diameter.

### *2.1. Modified-Alginate (mAlg)*

Sodium alginate was esterified with 1-decanol via Fisher esterification under mildly acid conditions (pH 4.0, adjusted with 1M HCl), following the procedure reported by Broderick, et al. [15], with slight modifications. The reaction was carried out for 72 h at room temperature under constant magnetic stirring. The product was purified by dialysis, freeze-dried, and stored at room temperature. Successful esterification was confirmed by FTIR-ATR spectroscopy.

### *2.2. Bacteria and Bacteriophage Strains*

*Escherichia coli* strains were obtained from the "Centro Regional de Control de Enfermedades Infecciosas" (CRCEI), School of Medicine, Universidad Autónoma de Nuevo León (UANL). These isolates were recovered from cystic fibrosis (CF) patients and had been previously characterized. Bacteriophage vB_Eco_K-02, previously characterized [16], was also provided by CRCEI and was isolated from the wastewater collected at the Hospital Universitario "Dr. José Eleuterio González" (School of Medicine, UANL).

### *2.3. Synthesis of mAlg-Cs Nanoparticles (mAlg-Cs NPs)*

Nanoparticles were prepared by electrostatic complexation between the two polysaccharides, assisted by ultrasonication. Briefly, a chitosan solution (0.2%, pH 5.0) was added dropwise into an aqueous mAlg solution (5 mL, 0.2% pH 4.5) under sonication using a probe sonicator (Q500 Sonicator, QSonica, Newtown, CT, USA) operated at 20% amplitude for 5 min. The amount of mAlg was kept constant across all formulations, while the volume of chitosan solution was varied to obtain mAlg:Cs mass ratios of 1:0.455, 1:0.500, 1:0.555, 1:0.625 and 1:0.710. After sonication, the colloidal suspensions were centrifuged at 7607 ×g for 30 min at 15 °C. The supernatant was discarded and the nanoparticles were resuspended in sterile water for further characterization.

### *2.4. Preparation of vB_Eco_K-02-Loaded Nanoparticles (mAlg-Cs-Phg)*

Phage-loaded nanoparticles were prepared using the same protocol. Briefly, a vB_Eco_K-02 aliquot (~$10^6$ plaque-forming units per milliliter, PFU/mL) was first mixed with the chitosan solution and then added dropwise to the mAlg solution under ultrasonication. After centrifugation, the supernatant was collected to quantify the encapsulation efficiency (%EE) and the nanoparticles were resuspended in sterile water for subsequent characterization.

### *2.5. Encapsulation Efficiency*

Encapsulation efficiency (EE) was calculated from the difference between the initial phage titer ($P_{Total}$) and free vB_Eco_K-02 phage titer in the supernatant ($P_{free}$), determined by the double-layer agar method. EE was calculated as:

$$\%EE = \frac{P_{Total} - P_{Free}}{P_{Total}} x100$$

 doi:10.20944/preprints202602.1251.v1



*2.6. Antibacterial Activity*

To assess the stability and the antibacterial activity of mAlg-Cs-Phg, they were exposed to different temperature conditions (37, 40, and 50 °C) and pH values (3 and 11). Samples were incubated for 48 h in a ThermoMixer C (300 rpm). Aliquots were collected after 24 h and analyzed by the double-layer agar method (drop) assay to evaluate phage-mediated bacterial lysis. vB_Eco_K-02 phage-positive suspensions were further tested in vitro by monitoring bacterial growth kinetics. For the growth inhibition assay, samples of LB broth (control), vB_Eco_K-02 suspension (1:100 dilution), mAlg-Cs nanoparticles, and mAlg-Cs-Phg nanoparticles were loaded in a 96-well microplate. An *E. coli* inoculum (OD = 0.1) was added to each well. Plates were incubated at 37 °C in a microplate reader (Multitskan sky, Thermoscientific), and $OD_{600}$ was recorded every 30 minutes for 12 hours. Experiments were performed in triplicate.

*2.7. FTIR-ATR Spectroscopy*

FTIR-ATR spectra were acquired using a PerkinElmer spectrophotometer (Connecticut, USA), over the range 4000 to 400 $cm^{-1}$ at a resolution of 2 $cm^{-1}$.

*2.8. Particle Size and Zeta Potential*

Hydrodynamic diameter and zeta potential were measured by dynamic light scattering (DLS) and electrophoretic light scattering using a Zeta Nano ZS (Malvern instruments), equipped with a 633 nm He-Ne laser (4mW). Measurements were performed in triplicate at 25 °C. Results are reported as mean ± standard deviation (n = 3); the number of sub-runs per measurement was set automatically by the instrument.

*2.9. Nanoparticle Morphology*

Nanoparticle morphology was examined by atomic force microscopy (AFM) using a JSPM-4210 instrument (JEOL) with a Mikromasch HQ:NSC15/Al BS cantilever with a nomina spring constant 40 N/m and a resonance frequency around 325 kHz. Images were obtained in non-contact mode. An aliquot of the nanoparticle suspension was deposited onto freshly cleaved mica. After 1-minute, excess liquid was removed with adsorbed paper, and the sample was allowed to air-dry prior to imaging.

## 3. Results

*3.1. Chemical Modification of Alginate*

The FTIR-ATR spectra of native alginate and modified alginate (mAlg) are shown in Figure 1. Both spectra show a broad -OH stretching band around 3500-3000 $cm^{-1}$ region, characteristic asymmetric and symmetric stretching vibrations of the carboxylate group --$COO^-$ at 1595 and 1407 $cm^{-1}$, respectively, and C-O-C stretching vibrations in the 1100-1000 $cm^{-1}$ region. Notably, an additional peak at 1733 $cm^{-1}$, assigned to the ester carbonyl (-C=O) stretching vibration, appears only in mAlg spectrum. These results confirm successful esterification of alginate and indicate the covalent incorporation of 1-decanol moieties via ester bond.

*3.2. Hydrodynamic Size and Zeta Potential of mAlg-Cs Nanoparticles*

Modified alginate-chitosan nanoparticles (mAlg-Cs Np) were synthesized by electrostatic complexation at different mAlg:Cs mass ratios. Table 1 summarizes the average hydrodynamic diameter ($D_H$), polydispersity index and zeta potential (ζP) for the formulations (1:0.455, 1:0.500, 1:0.550, 1:0.625, and 1:0.710). As the chitosan fraction increased from 1:0.455 to 1:0.625, the particle size progressively decreased from 749 nm to 631 nm and the PDI narrowed from 0.351 to 0.295, indicating improved colloidal uniformity. Within this range, ζP remained essentially constant (ca. -41 to -42 mV), suggesting that particle surface composition is dominated by anionic mAlg. At the

 doi:10.20944/preprints202602.1251.v1



highest chitosan content (1:0.710), both the hydrodynamic size (651 nm) and ζP (-38 mV) shifted, consistent with partial enrichment of chitosan in the outer shell, which slightly alter the surface composition.

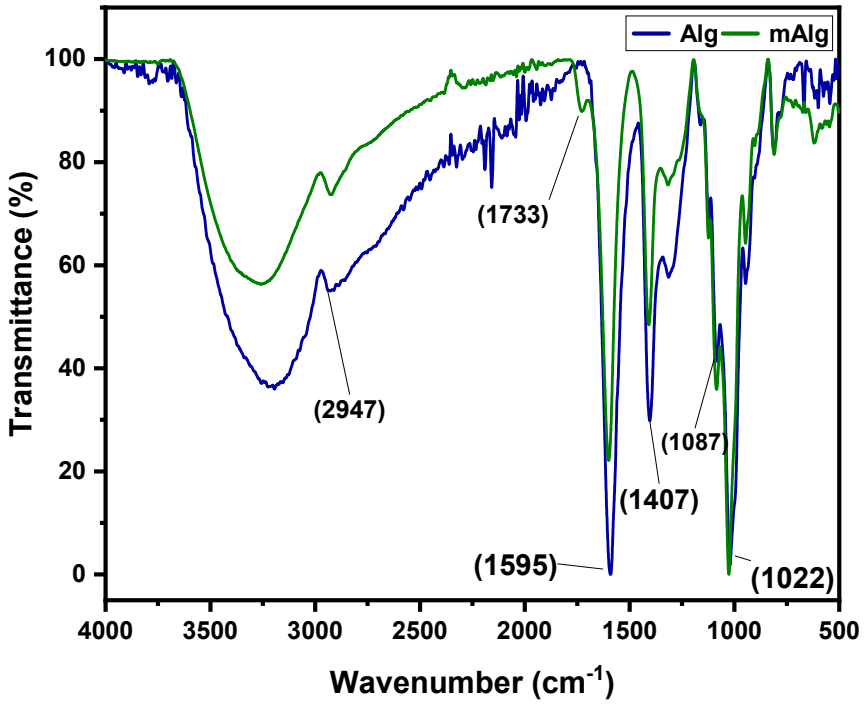


**Figure 1.** FTIR-ATR spectra of native Alg (blue) and mAlg (green).

**Table 1.** $D_H$, PDI, and ζP of mAlg:Cs particles prepared at different biopolymers mass ratios. Values are mean ± SD (n = 5).

| mAlg:Cs | $D_H$ (nm) | PDI | ζP (mV) |
|---|---|---|---|
| **1:0.455** | 749 ± 8 | 0.351 | -42 ± 1 |
| **1:0.500** | 690 ± 18 | 0.310 | -41 ± 2 |
| **1:0.550** | 649 ± 9 | 0.304 | -42 ± 1 |
| **1:0.625** | 631 ± 8 | 0.295 | -42 ± 0.5 |
| **1:0.710** | 651 ± 23 | 0.300 | -38 ± 1 |

AFM images (Figure 2) showed that mAlg-Cs particles prepared at ratios up to 1:0.625 showed predominantly regular ovoid morphologies, whereas the 1:0.710 formulation showed irregular particles shapes. Considering the size, ζP, and morphology, the 1:0.625 mAlg:Cs formulation was selected as the optimal polymeric matrix for phage loading.

*3.3. Bacteriophage-Loaded mAlg-Cs Nanoparticles*

The 1:0.625 mAlg-Cs formulation showed a high capacity for encapsulating the vB_Eco_K-02. The physicochemical properties of unloaded and phage-loaded particles (mAlg-Cs-Phg) are summarized in Table 2. Interestingly, phage-loading reduces the $D_H$ of nanoparticles from 631 nm to 538 nm. Meanwhile, the ζP remained essentially unchanged at approximately -42 mV. AFM analysis supported this trend, with the apparent ovoid dimension decreasing from approximately 180 × 300 nm (unloaded particle) to 140 × 220 nm (mAlg-Cs-Phg particle) (Figure 3). Collectively, these results suggest that virions may act as templates, promoting Cs adsorption onto the phage surface prior to complexation with mAlg, thereby yielding a more ordered assembly and smaller particles.

 doi:10.20944/preprints202602.1251.v1



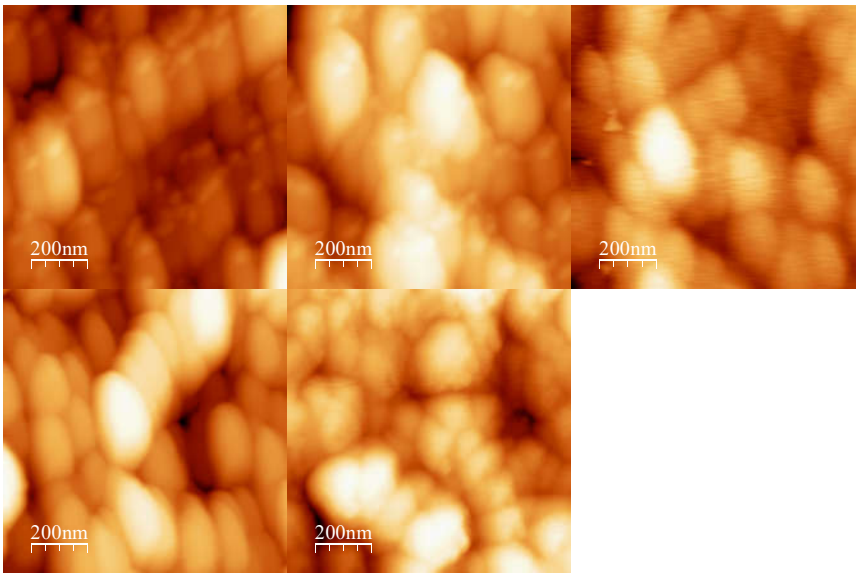


**Figure 2.** AFM micrographs of mAlg-Cs particles at mAlg:Cs ratios a) 1:0.455, b) 1:0.500, c)1:0.550, d) 1:0.625, and e) 1:0.710.

**Table 2.** Comparation of $D_H$, PDI, ζP, polydispersity index and zeta potential for unloaded and phage loaded mAlg-Cs particles (mAlg:Cs = 1:0.625). Values are mean ± SD (n = 5).

| Sample | $D_H$ (nm) | PDI | ζP (mV) |
|---|---|---|---|
| **mAlg-Cs 1:0.625** | 631 ± 8 | 0.295 | -42 ± 0.5 |
| **mAlg-Cs-Phg 1:0.625** | 538 ± 8 | 0.279 | -42 ± 0.5 |

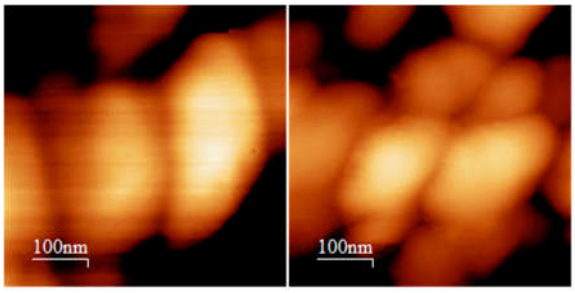


**Figure 3.** AFM micrographs of a) mAlg-Cs particles and b) mAlg-Cs-Phg particles.

*3.4. Encapsulation Efficiency*

Encapsulation efficiency was estimated indirectly by quantifying free vB_Eco_K-02 in the supernatant recovered after centrifugation of the mAlg-Cs-Phg NPs suspension. The supernatant titer was compared with the initial phage input (~$10^6$ PFU/mL). The double-layer agar assay showed ~$10^3$ PFU/mL in the supernatant, corresponding to an encapsulation efficiency of approximately 99% (Figure 4). These results demonstrate that mAlg-Cs matrix is highly effective for phage loading.

*3.5. Antibacterial Activity Phage-Loaded mAlg-Cs Nasnoparticles*

After formulation, the lytic activity of mAlg-Cs-Phg particles was evaluated against *E. coli* isolated from CF patients. As an initial assessment, freshly prepared mAlg-Cs-Phg suspensions (pH 5.5) were tested at room temperature. However, no plaques or lysis zones were observed by the double-layer agar assay (data not shown). This suggests that phages were strongly retained within the mAlg-Cs matrix under these conditions, limiting their immediate release.

 doi:10.20944/preprints202602.1251.v1



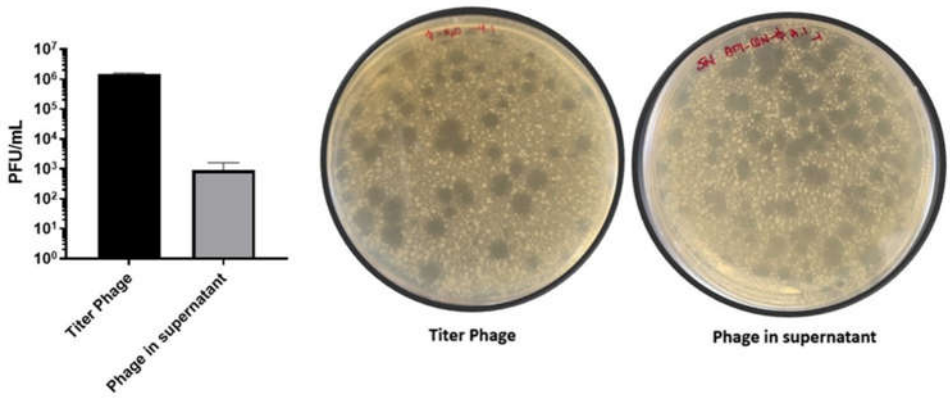


**Figure 4.** Encapsulation efficiency and lytic activity of free phage before and after encapsulation in mAlg-Cs nanoparticles. a) Phage titer comparison between the initial phage concentration (~$10^6$ PFU/mL) and free phages collected in the supernatant (~$10^3$ PFU/mL), yielding approximately 99% encapsulation efficiency. b) Representative agar plates showing lysis after serial dilution ($10^0$ - $10^{-10}$). For plating, 100 µL of diluted samples were mixed with soft LB agar and poured onto solid LB agar, followed by incubation at 37 °C for 18 hrs. PFU/mL was calculated from plaque counts using plated volume and dilution factor.

Therefore, additional experiments were performed to study the influence of pH and temperature on phage release and lytic activity. Under alkaline conditions (pH 11.0), mAlg-Cs-Phg particles exhibited detectable lytic activity after 24 h of incubation at 37 °C and 40 °C (Figure 5), whereas no antibacterial activity was observed at 50 °C or acidic pH (pH 3.0). These results define a functional stability window for encapsulated phages and indicate that extreme acidity or elevated temperature compromises the viral activity.

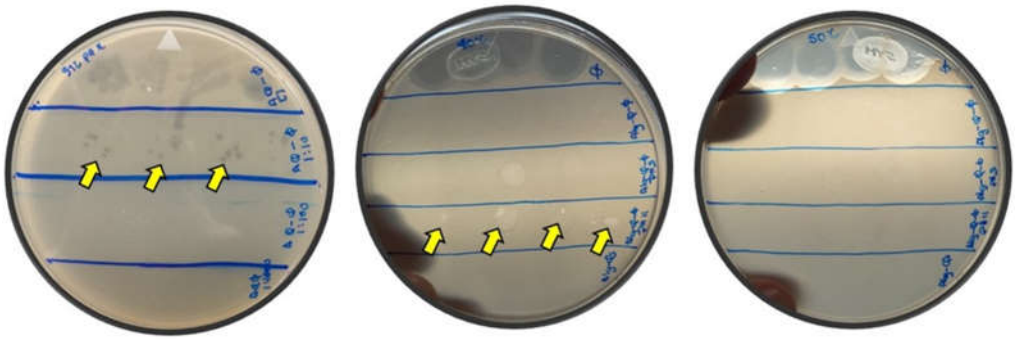

**Figure 5.** Representative agar plates showing antibacterial activity of phage-loaded particles under different pH and temperature conditions. Clear lysis zones (yellow arrows) were observed after incubation at 37 °C and 40 °C at pH 11.0, where no lysis was detected at 50 °C or at pH 3.0.

Based on these results, the condition that yielded lytic activity (37 °C and pH 11) was selected to evaluate bacterial growth kinetics. Four treatments were tested in a 96-well microplate: LB broth (control), free vB_Eco_K-02 phage, mAlg-Cs NPs and mAlg-Cs-Phg NPs. *E. coli* was added to each well (initial OD = 0.1), and growth was monitored at 37 °C by measuring $OD_{600}$ every 30 min for 12 h (Figure 6). In the absence of phage, *E. coli* shows a lag phase (0 – 3 h), followed by exponential growth (3 – 7 h) and reaching the stationary phase. Unloaded mAlg-Cs NPs slightly altered the growth profile, shortening the exponential phase. In contrast, both free vB_Eco_K-02 and mAlg-Cs-Phg NPs fully suppressed measurable growth over the experimental time assay, indicating that phages retained lytic activity after encapsulation and could effectively inhibit proliferation under the tested conditions.

 doi:10.20944/preprints202602.1251.v1



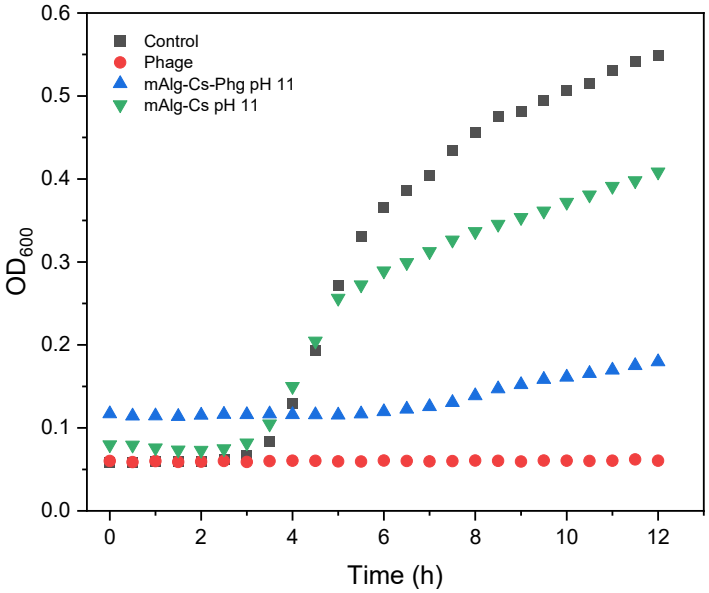


**Figure 6.** *E. coli* growth kinetics monitored by $OD_{600}$ over 12 h at 37 °C. Treatments included LB broth (positive control), free phage (~$10^5$ PFU/mL; negative growth control), unloaded mAlg-Cs NPs (pH 11), and phage loaded mAlg-Cs NPs (pH 11). Initial bacterial density: $OD_{600}$ = 0.1 (~1x$10^8$ CFU). No detectable growth was observed in the presence of free phage of mAlg-Cs-Phg NPs, confirming preserved antibacterial activity after encapsulation.

## 4. Discussion

Alginate esterification was successfully achieved through covalent attachment of 1-decanol. FTIR spectra confirmed the modification by comparison of the characteristic bands of pristine alginate and modified alginate (mAlg). In particular, the mAlg spectrum showed a new peak near 1700 $cm^{-1}$, attributable to ester carbonyl (-C=O) stretching, consistent with the formation of ester linkages between -OH group of 1-decanol and -COOH groups on the alginate backbone [17]. Introducing hydrophobic alkyl chains is expected to alter alginate physicochemical properties (solubility and gelation behavior), which can facilitate nanoparticle formation[18] and improve encapsulation of peptides, proteins, and other bioactive compounds, thereby broadening drug-delivery applications of this natural polysaccharides [19,20].

In aqueous media, alginate and chitosan carry opposite charges due to their ionizable functional groups, enabling the formation of polyelectrolyte complexes through electrostatic interaction. Accordingly, chemical modification of alginate can influence its complexation with chitosan (Cs) and promote the formation of stable nanoparticles [21,22]. Moreover, alginate-chitosan systems have been widely explored as carrier matrices for drugs, proteins, and biological agents such as bacteriophages. Bacteriophages are viruses that specifically infect prokaryotic cells and represent a promising alternative for treating infections caused by MDR bacteria [23].

Based on these considerations, mAlg:Cs NPs were engineered as phage-loading and delivery platform. The nanoparticles were produced by electrostatic complexation at different biopolymers mass ratios, with ultrasonication assisting assembly and reducing aggregation. Based on DLS, ζP, and AFM results, the 1:0.625 mAlg:Cs formulation generated particles with the most favorable size distribution and morphology. Considering the approximate size of vB_Eco_K-02 (160 nm [16]), the nanoparticle dimensions suggest that multiple virions could be accommodated within nanoparticle. In addition, the strongly negative ζP (-42 mV) is consistent with the good colloidal stability of the suspension [24,25].

Notably, relative to unloaded mAlg:Cs NPs, vB_Eco_K-02-loaded NPs exhibited a reduced hydrodynamic diameter (from 630 nm to 537 nm). This decrease suggests that virions may act as nanoscale scaffolds that promotes chitosan adsorption onto the phage surface, followed by the

 doi:10.20944/preprints202602.1251.v1



deposition of mAlg onto the Cs -coated phage, yielding a more compact and organized nanostructure as compared to the unloaded particles.

The mAlg:Cs matrix showed excellent phage loading performance, as evidenced by the high encapsulation efficiency (EE ~99%). Since the recovered supernatant contained ~$10^3$ PFU/mL, the vast majority of phages from the initial titer (~$10^6$ PFU/mL) were effectively incorporated into the mAlg:Cs NPs. This high EE suggests strong interactions between positively charged chitosan chains and negatively charged regions on the phage surface. This suggests that preformed phage-Cs complexes may serve as templates for the subsequent ionic adsorption of mAlg. Moreover, hydrophobic interaction between the alkyl chains of mAlg may further drive the formation of a compact polyanionic shell around the preformed phage-Cs cores. In addition, hydrophobic modification with 1-decanol may influence mAlg chain conformation and interpolymer packing, favoring adsorption onto the phage-Cs complex, increasing structural compactness, and decreasing network permeability. Together, these effects could reduce premature phage release. the structural compactness and decreasing the permeability of the polymeric network, thereby reducing phage release. Comparable EE values have been reported for related polysaccharide-based systems in which polyelectrolyte complexation provides a favorable microenvironment for viral or proteinaceous cargo [13,26,27]. Furthermore, the mild aqueous processing conditions and absence of organic solvents has contributed to preserving phage viability during formulation [7,26]. Overall, the 99% EE observed here highlights the effectiveness of the alginate–chitosan matrix as both a protective barrier and potential controlled-release carrier for bacteriophages.

Given the high EE, it is expected to be strong antibacterial activity under standard culture conditions. However, when tested against *E. coli* strain isolated from cystic fibrosis patients at 37 °C and 7.4 pH, the nanosystem showed limited activity, consistent with negligible lytic activity detected in the double-layer agar assay. Two hypotheses could explain this behavior: (i) partial loss of phage infectivity due to ultrasonication, or (ii) an excessively strong retention of phages within the polymeric matrix that prevented their release into the medium. The first scenario is hardly probably because the recovered supernatant exhibited clear lytic activity, indicating that ultrasonication was sufficiently gentle to preserve virion infectivity. Therefore, the hypothesis of a strong entrapment within the polymeric network is the most plausible explanation.

To address this limitation, additional experiments were performed to identify incubation conditions (temperature and pH) that promote phage release from mAlg:Cs matrix. Interestingly, phage-loaded nanoparticles showed detectable lytic activity under alkaline conditions (pH 11.0) at 37 °C and 40 °C, further supporting that ultrasonication did not compromise phage activity. In contrast, no lysis was observed under the other tested conditions (50 °C and pH 11.0; 37, 40 and 50 °C at pH 7.4 or 3.0), consistent with the thermal sensitivity and reduced stability of many phages at elevated temperature and under acidic conditions [16]. Collectively, these findings indicate that encapsulation preserves infectivity and may provide moderate protection against environmental stressors, potentially extending usability across relevant storage and handling conditions.

The doble-layer agar-based results were corroborated by growth kinetics ($OD_{600}$) over 12 h. Under the selected condition (37 °C, pH 11.0), mAlg-Cs-Phg NPs strongly inhibited *E. coli* growth throughout the incubation period. In contrast, unloaded nanoparticles (mAlg-Cs NPs) produced a modest effect, mainly shortening the exponential growth phase. These results indicate that antibacterial activity is driven by encapsulated phage rather than the biopolymeric matrix. Sustained growth suppression is also consistent with time-dependent release of active phages from the nanoparticle system, maintaining inhibitory action during the assay.

Overall, these results demonstrate the potential of mAlg-Cs-Phg NPs as a delivery platform for bacteriophages, providing protection against environmental stress and enabling sustained antibacterial activity. Prior studies have reported phage encapsulation and bactericidal effects using polysaccharide-based carriers, although polymer architectures and length scales differ from the present formulation [13,26,28–30]. For instance, Abdelsattar et al. encapsulated phages in an alginate matrix coated with chitosan, reporting improved protection in acidic conditions and reduced

 doi:10.20944/preprints202602.1251.v1



bacterial viability under simulated intestinal conditions. That system used microscale beads with relatively large pores, whereas nanoscale carriers typically exhibit tighter polymer networks that can enable more controlled release. Similarly, Kaur et al. reported alginate-Cs nanoparticles for endolysin delivery, achieving controlled release and enhanced antibacterial activity. In this context, the nanosystem developed here combines efficient vB_Eco_K_02 encapsulation, partial protection under harsh conditions, and sustained antibacterial effects. Nevertheless, further studies are required to fully validate performance, including quantitative phage release profiling, evaluation of phage stability over time, and determination of multiplicity of infection, which are critical to link release kinetics with antibacterial efficacy.

## 5. Conclusions

Polysaccharide-based nanoparticles composed of hydrophobically modified alginate and chitosan were developed as a cargo matrix for bacteriophage vB_Eco_K_02. Among the formulations prepared by varying pH of the mAlg and Cs solutions and the polymer mass ratio, the 1:0.625 mAlg-Cs formulation yielded nanoparticles with the most favorable physicochemical properties, including narrowed size distribution, high colloidal stability, and regular morphology. Importantly, phage-loaded mAlg-Cs NPs achieved a high encapsulation efficiency (99%) and preserved vB_Eco_K_02 lytic activity after formulation, resulting in strong inhibition of *E. coli* growth in kinetic assays. Interestingly, the mAlg–Cs–Phg system exhibited enhanced antibacterial activity at pH 11 and 37 °C. While these conditions deviate from physiological pH, they are clinically relevant in specific medical scenarios, most notably in endodontic therapy. During root canal treatments, calcium hydroxide is the gold standard medication, creating a highly alkaline environment (pH 11–12.5) to eliminate persistent pathogens. The superior performance of our phage-loaded nanoparticles under these conditions suggests they could serve as a potent adjunct to intracanal disinfection, overcoming the alkalinity that often inactivates conventional biological agents. Furthermore, such alkaline resilience is valuable for treating chronic infected wounds, where the formation of bacterial biofilms can shift the local microenvironment toward alkaline values (pH 8.5–10.5). Therefore, the mAlg–Cs matrix not only stabilizes the bacteriophages but also potentially potentiates their lytic activity in alkaline clinical niches where antibiotic efficacy is often compromised. Overall, mAlg-Cs nanoparticles provide an efficient platform for vB_Eco_K_02 encapsulation, maintaining phage infectivity and enabling effective antibacterial activity. This nanosystem represents a promising strategy to enhance phage delivery for the treatment of bacterial infection.

**Author Contributions:** Conceptualization, J.J., A.T., and D.E.; methodology, P.D.M.F., J.A.G.M., J.M.G.P.; validation, G.G., G.R. and M.A.L.M.; formal analysis, J.J., A.T., D.E., G.G., G.R. and M.A.L.M.; investigation, J.J., A.T., P.D.M.F., J.A.G.M., J.M.G.P.; resources, J.J.; data curation, J.J., D.E.; writing—original draft preparation, J.J., and P.D.M.F.; writing—review and editing, J.J.; visualization, J.J.; supervision, J.J., A.T., D.E., G.G., G.R. and M.A.L.M.; project administration, J.J.; funding acquisition, J.J., A.T., D.E., G.G., G.R. and M.A.L.M. All authors have read and agreed to the published version of the manuscript. Please turn to the CRediT taxonomy for the term explanation. Authorship must be limited to those who have contributed substantially to the work reported.

**Funding:** This research was funded by SECIHTY under project CF-2023-G041. PhD students P.D.M.F. and J.A.G.M. acknowledge SECIHTI for the doctoral scholarship (grant number 1009922 and 1078311).

**Acknowledgments:** The Authors gratefully acknowledge SECIHTI for financial support of this work. P.D.M.F. and J.A.G.M. also acknowledge SECIHTI for the doctoral scholarships (grant number XXX).

**Conflicts of Interest:** The authors declare no conflicts of interest.

## References

1. *WHO Bacterial Priority Pathogens List , 2024*. 2024.

 doi:10.20944/preprints202602.1251.v1




2. J. J. Iszatt, A. N. Larcombe, H. Chan, S. M. Stick, L. W. Garratt, and A. Kicic, "Phage Therapy for Multi-Drug Resistant Respiratory Tract Infections," pp. 1–14, 2021, doi: 10.3390/v13091809.
3. Z. Chegini, A. Khoshbayan, M. Taati Moghadam, I. Farahani, P. Jazireian, and A. Shariati, "Bacteriophage therapy against Pseudomonas aeruginosa biofilms: A review," *Ann. Clin. Microbiol. Antimicrob.*, vol. 19, no. 1, pp. 1–17, 2020, doi: 10.1186/s12941-020-00389-5.
4. M. Wdowiak, J. Paczesny, and S. Raza, "Enhancing the Stability of Bacteriophages Using Physical, Chemical, and Nano-Based Approaches: A Review," *Pharmaceutics*, vol. 14, no. 9, 2022, doi: 10.3390/pharmaceutics14091936.
5. S. S. Y. Leung et al., "Effects of storage conditions on the stability of spray dried, inhalable bacteriophage powders," *Int. J. Pharm.*, vol. 521, no. 1–2, pp. 141–149, 2017, doi: 10.1016/j.ijpharm.2017.01.060.
6. A. M. Pinto, M. D. Silva, L. M. Pastrana, M. Bañobre-López, and S. Sillankorva, "The clinical path to deliver encapsulated phages and lysins," *FEMS Microbiol. Rev.*, vol. 45, no. 5, pp. 1–29, 2021, doi: 10.1093/femsre/fuab019.
7. B. Loh, V. S. Gondil, P. Manohar, F. M. Khan, H. Yang, and S. Leptihn, "Encapsulation and Delivery of Therapeutic Phages," *Appl. Environ. Microbiol.*, vol. 87, no. 5, pp. 1–13, 2021, doi: 10.1128/AEM.01979-20.
8. J. García-Mar et al., "Engineering of ICG-doxorubicin-loaded alginate-chitosan nanoparticles for gynecological cancer chemo-phototherapy," *Int. J. Biol. Macromol.*, vol. 328, no. June, p. 147554, 2025, doi: 10.1016/j.ijbiomac.2025.147554.
9. S. A. Elghobashy, A. B. Abeer Mohammed, A. A. Tayel, F. A. Alshubaily, and A. Abdella, "Thyme/garlic essential oils loaded chitosan-alginate nanocomposite: Characterization and antibacterial activities," *E-Polymers*, vol. 22, no. 1, pp. 997–1006, 2022, doi: 10.1515/epoly-2022-0090.
10. T. Nalini, S. K. Basha, A. M. Sadiq, and V. S. Kumari, "In vitro cytocompatibility assessment and antibacterial effects of quercetin encapsulated alginate/chitosan nanoparticle," *Int. J. Biol. Macromol.*, vol. 219, no. August, pp. 304–311, 2022, doi: 10.1016/j.ijbiomac.2022.08.007.
11. K. K. Patel et al., "Alginate lyase immobilized chitosan nanoparticles of ciprofloxacin for the improved antimicrobial activity against the biofilm associated mucoid *P. aeruginosa* infection in cystic fibrosis," *Int. J. Pharm.*, vol. 563, no. March, pp. 30–42, 2019, doi: 10.1016/j.ijpharm.2019.03.051.
12. M. Hill et al., "Alginate/chitosan particle-based drug delivery systems for pulmonary applications," *Pharmaceutics*, vol. 11, no. 8, pp. 1–12, 2019, doi: 10.3390/pharmaceutics11080379.
13. L. Silva Batalha et al., "Encapsulation in alginate-polymers improves stability and allows controlled release of the UFV-AREG1 bacteriophage," *Food Res. Int.*, vol. 139, no. December 2020, 2021, doi: 10.1016/j.foodres.2020.109947.
14. D. J. Malik, "Approaches for manufacture, formulation, targeted delivery and controlled release of phage-based therapeutics," *Curr. Opin. Biotechnol.*, vol. 68, pp. 262–271, 2021, doi: 10.1016/j.copbio.2021.02.009.
15. E. Broderick, H. Lyons, T. Pembroke, H. Byrne, B. Murray, and M. Hall, "The characterisation of a novel, covalently modified, amphiphilic alginate derivative, which retains gelling and non-toxic properties," *J. Colloid Interface Sci.*, vol. 298, no. 1, pp. 154–161, 2006, doi: 10.1016/j.jcis.2005.12.026.
16. G. García-González et al., "Isolation and Characterization of Four New Coliphages against Extra Intestinal Pathogenic *Escherichia coli* Isolates Recovered from Cystic Fibrosis Patients," *ACS Omega*, vol. 10, no. 40, pp. 46704–46713, 2025, doi: 10.1021/acsomega.5c04140.
17. N. Mor and N. Raghav, "In-vitro simulation of modified-alginate ester as sustained release delivery system for curcumin," *J. Mol. Struct.*, vol. 1283, 2023, doi: 10.1016/j.molstruc.2023.135307.
18. P. Yan, W. Lan, and J. Xie, "Modification on sodium alginate for food preservation: A review," *Trends Food Sci. Technol.*, vol. 143, no. July 2023, p. 104217, 2024, doi: 10.1016/j.tifs.2023.104217.
19. E. Rostami, "Recent achievements in sodium alginate - based nanoparticles for targeted drug delivery," *Polym. Bull.*, no. 0123456789, 2021, doi: 10.1007/s00289-021-03781-z.
20. F. Moghtader, S. Solakoglu, and E. Piskin, "Alginate- and Chitosan-Modified Gelatin Hydrogel Microbeads for Delivery of *E. coli* Phages," *Gels*, vol. 10, no. 4, 2024, doi: 10.3390/gels10040244.
21. D. Wu et al., "Chitosan-based Colloidal Polyelectrolyte Complexes for Drug Delivery: A Review," *Carbohydr. Polym.*, vol. 238, no. March, 2020, doi: 10.1016/j.carbpol.2020.116126.

 doi:10.20944/preprints202602.1251.v1




22. Y. Luo and Q. Wang, "Recent development of chitosan-based polyelectrolyte complexes with natural polysaccharides for drug delivery," *Int. J. Biol. Macromol.*, vol. 64, pp. 353–367, 2014, doi: 10.1016/j.ijbiomac.2013.12.017.
23. P. Hyman and J. Denyes, *Bacteriophages in Nanotechnology: History and Future*. 2021.
24. T. Yilmaz, L. Maldonado, H. Turasan, and J. Kokini, "Thermodynamic mechanism of particulation of sodium alginate and chitosan polyelectrolyte complexes as a function of charge ratio and order of addition," *J. Food Eng.*, vol. 254, no. November 2018, pp. 42–50, 2019, doi: 10.1016/j.jfoodeng.2019.03.002.
25. S. Bhattacharjee, "DLS and zeta potential - What they are and what they are not?," *J. Control. Release*, vol. 235, pp. 337–351, 2016, doi: 10.1016/j.jconrel.2016.06.017.
26. M. M. Elsayed, R. M. Elkenany, A. Y. EL-Khateeb, N. M. Nabil, M. M. Tawakol, and H. M. Hassan, "Isolation and encapsulation of bacteriophage with chitosan nanoparticles for biocontrol of multidrug-resistant methicillin-resistant *Staphylococcus aureus* isolated from broiler poultry farms," *Sci. Rep.*, vol. 14, no. 1, pp. 1–12, 2024, doi: 10.1038/s41598-024-55114-5.
27. A. S. Abdelsattar, F. Abdelrahman, A. Dawoud, I. F. Connerton, and A. El-Shibiny, "Encapsulation of *E. coli* phage ZCEC5 in chitosan–alginate beads as a delivery system in phage therapy," *AMB Express*, vol. 9, no. 1, 2019, doi: 10.1186/s13568-019-0810-9.
28. J. Kaur, A. Kour, J. J. Panda, K. Harjai, and S. Chhibber, "Exploring Endolysin-Loaded Alginate-Chitosan Nanoparticles as Future Remedy for Staphylococcal Infections," *AAPS PharmSciTech*, vol. 21, no. 6, pp. 1–15, 2020, doi: 10.1208/s12249-020-01763-4.
29. S. G. Rotman et al., "Alginate chitosan microbeads and thermos-responsive hyaluronic acid hydrogel for phage delivery," *J. Drug Deliv. Sci. Technol.*, vol. 79, no. October 2022, p. 103991, 2023, doi: 10.1016/j.jddst.2022.103991.
30. Y. Zhou, D. Xu, H. Yu, J. Han, W. Liu, and D. Qu, "Encapsulation of Salmonella phage SL01 in alginate/carrageenan microcapsules as a delivery system and its application in vitro," *Front. Microbiol.*, vol. 13, no. August, pp. 1–11, 2022, doi: 10.3389/fmicb.2022.906103.